3D Rigid Body Impact Burial Prediction Model (IMPACT35)

Peter C Chu and Chenwu Fan
Naval Ocean Analysis and Prediction Laboratory, Oceanography Department
Naval Postgraduate School, Monterey, California, USA

Abstract

Falling of rigid body through air, water, and sediment is investigated experimentally and theoretically. Two experiments were conducted to drop rigid cylinders with the density ratio around 1.8 into shallow water (around 13 m deep) in the Monterey Bay (Exp-1) and into the Naval Postgraduate School's swimming pool (Exp-2). During the experiments, we carefully observe cylinder track and burial depth while simultaneously taking gravity cores (in Exp-1). After analyzing the gravity cores, we obtain the bottom sediment density and shear strength profiles. The theoretical work includes the development of 3D rigid body impact burial prediction model (IMPACT35) which contains three components: triple coordinate transform, hydrodynamics of falling rigid object in a single medium (air, water, or sediment) and in multiple media (air-water and water-sediment interfaces). The model predicts the rigid body's trajectory in the water column and burial depth and orientation in the sediment. The experimental data (burial depth, sediment density and shear strength) are used to evaluate the newly developed numerical model. The 3D model shows great improvement to the currently used US Navy's 2D model (i.e., IMPACT28).

1. Introduction

Study on falling rigid body through air, water, and sediment has wide scientific significance and technical application. The dynamics of a rigid body allows

one to set up six nonlinear equations for the most general motion: three momentum equations and three moment-of-momentum equations. The scientific studies of the geotechnical characteristics of a rigid body in water and sediment involve nonlinear dynamics, body and multi-phase fluid interaction, body-sediment interaction, and instability theory.

The technical application of the hydrodynamics of a rigid body into fluid and non-fluid includes aeronautics, navigation, and civil engineering. Recently, the scientific problem about the movement of a rigid body in water column and sediment drew attention to the naval research. This is due to the threat of mine in the Naval operations. Prediction of a falling rigid body in the water column provides an initial condition to determining the impact speed and direction of mine on the sediment and in turn in determining its burial depth and orientation. In this study, a nonlinear dynamical system is established for the movement of a nonuniform (center of gravity not the same as the center of volume) rigid cylinder through the water-sediment interface. A cylinder-drop experiment was conducted. The data collected from the experiment can be used for model development and verification.

2. Triple Coordinate Systems

Consider an axially symmetric cylinder with the centers of mass (**Mc**) and volume (**Gc**) on the main axis (Fig. 1). Let (L, d, χ) represent the cylinder's length, diameter, and the distance between the two points (**Mc**, **Gc**). The positive χ -values refer to nose-down case, i.e., the point **Mc** is lower than the point **Gc**. Three coordinate systems are used to model the falling cylinder through the air, water, and sediment phases: E-, M-, and F-coordinate systems. All the systems are three-dimensional, orthogonal, and right-handed (Chu et al., 2003).

The E-coordinate is represented by F_E(O, **i**, **j**, **k**) with the origin 'O', and three axes: x-, y- axes (horizontal) with the unit vectors (**i**, **j**) and z-axis (vertical) with the unit vector **k** (upward positive). The position of the cylinder is represented by the position of **Mc**,

$$\mathbf{X} = x\mathbf{i} + y\mathbf{j} + z\mathbf{k}, \tag{1}$$

which is translation of the cylinder. The translation velocity is given by

$$\frac{d\mathbf{X}}{dt} = \mathbf{V}, \qquad \mathbf{V} = (u, v, w). \tag{2}$$

Let orientation of the cylinder's main-axis (pointing downward) is given by $\mathbf{i}_M$. The unit vectors of the M-coordinate system are given by (Fig. 2)

$$\mathbf{j}_M = \mathbf{k} \times \mathbf{i}_M, \qquad \mathbf{k}_M = \mathbf{i}_M \times \mathbf{j}_M \tag{3}$$

Let the cylinder rotate around ($\mathbf{i}_M$, $\mathbf{j}_M$, $\mathbf{k}_M$) with angles ($\varphi_1, \varphi_2, \varphi_3$) (Fig. 2). The angular velocity of cylinder is calculated by

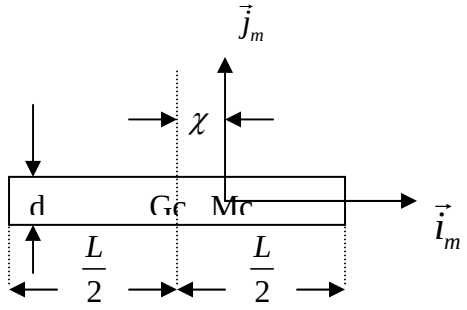

Fig. 1. M-coordinate with the COM as the origin X and (i_m, j_m) as the two axes. Here, χ is the distance between the COV (B) and COM, (*L*, *d*) are the cylinder's length and diameter.

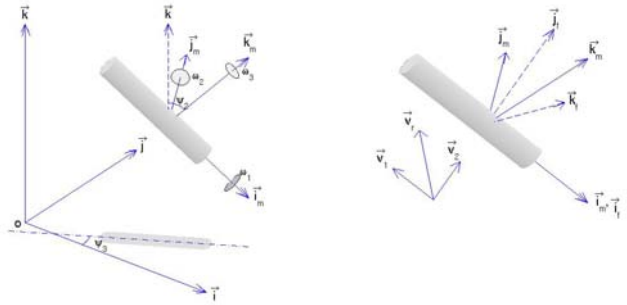

Fig. 2. Three coordinate systems.

$$\omega_1 = \frac{d\varphi_1}{dt}, \quad \omega_2 = \frac{d\varphi_2}{dt}, \quad \omega_3 = \frac{d\varphi_3}{dt}. \tag{4}$$

The F-coordinate is represented by F_F(**X**, $\mathbf{i}_F$, $\mathbf{j}_F$, $\mathbf{k}_F$) with the origin **X**, unit vectors ($\mathbf{i}_F$, $\mathbf{j}_F$, $\mathbf{k}_F$), and coordinates (x_F, y_F, z_F). Let $\mathbf{V}_w$ be the fluid velocity. The water-to-cylinder velocity is represented by

$$\mathbf{V}_r = \mathbf{V}_w - \mathbf{V},$$

which can be decomposed into two parts,

$$\mathbf{V}_r = \mathbf{V}_1 + \mathbf{V}_2, \quad \mathbf{V}_1 = (\mathbf{V}_r \cdot \mathbf{i}_F)\mathbf{i}_F, \quad \mathbf{V}_2 = \mathbf{V}_r - (\mathbf{V}_r \cdot \mathbf{i}_F)\mathbf{i}_F, \tag{5}$$

where $\mathbf{V}_1$ is the component paralleling to the cylinder's main-axis (i.e., along $\mathbf{i}_M$), and $\mathbf{V}_2$ is the component perpendicular to the cylinder's main-axial direction. The unit vectors for the F-coordinate are defined by (column vectors)

$$\mathbf{i}_F = \mathbf{i}_M, \qquad \mathbf{j}_F = \mathbf{V}_2/|\mathbf{V}_2|, \qquad \mathbf{k}_F = \mathbf{i}_F \times \mathbf{j}_F. \tag{6}$$

3. Momentum Balance

The translation velocity of the cylinder (**V**) is governed by the momentum equation in the E-coordinate system,

$$\frac{d}{dt}\begin{bmatrix} u \\ v \\ w \end{bmatrix} = -\begin{bmatrix} 0 \\ 0 \\ g-b \end{bmatrix} + \frac{1}{\rho\Pi}\mathbf{F}_h, \tag{7}$$

where g is the gravitational acceleration; b is the buoyancy force; Π is the cylinder volume; ρ is the rigid body density; $\rho\Pi = m$, is the cylinder mass; $\mathbf{F}_h$ is the hydrodynamic force (including drag, lift, impact forces). The drag and lift forces are calculated using the drag and lift laws with the given water-to-cylinder velocity ($\mathbf{V}_r$). In the F-coordinate, $\mathbf{V}_r$ is decomposed into along-cylinder ($\mathbf{V}_1$) and across-cylinder ($\mathbf{V}_2$) components.

4. Moment of Momentum Equation

It is convenient to write the moment of momentum equation

$$\mathbf{J} \cdot \frac{d\boldsymbol{\omega}}{dt} = \mathbf{M}_b + \mathbf{M}_h, \tag{8}$$

in the M-coordinate system with the cylinder's angular velocity components ($\omega_1, \omega_2, \omega_3$) defined by (4). Here, $\mathbf{M}_b$ and $\mathbf{M}_h$ are the body and surface (hydrodynamic) force torques. In the M-coordinate system, the moment of gyration tensor for the axially symmetric cylinder is a diagonal matrix

$$\mathbf{J} = \begin{bmatrix} J_1 & 0 & 0 \\ 0 & J_2 & 0 \\ 0 & 0 & J_3 \end{bmatrix}, \tag{9}$$

where J_1, J_2, and J_3 are the moments of inertia. The gravity force, passing the center of mass, doesn't induce the moment.

5. Three Sub-Cylinders

Penetration of cylindrical body into air-water and water-sediment interface is quite complicated. For simplicity, the cylinder is divided into three sub-cylinders: Cylinder-1, Cylinder-2, and Cylinder-mix. Cylinder-1 and Cylinder-2 are the sub-cylinders contacting with only one medium (air, water, or sediment). However, Cylinder-mix is the middle part o contacting two adjacent media (air-water or water-sediment). Here, we use the water-sediment interface as an illustration.

Cylinder-mix for penetrating the water-sediment interface is divided it into two parts: wet cut-off (contacting water) and dry cut-off (contacting sediment). For computing ($\mathbf{F}_h$, $\mathbf{M}_h$) on the wet cut-off part, an equivalent cylinder is proposed for the wet cut-off part in such a way that the centers of mass and volume for the whole cylinder (**Mc, Gc**), and center of volume for the water-covered area ($\mathbf{Gc}_w$, i.e., the volume center of the combination of the cylinder-1 and wet cut-off) are kept the same with the original cylinder (Fig. 3). The hydrodynamic forcing for the water-sediment interface is computed by

$$\mathbf{F}_h = \mathbf{F}_s + \mathbf{F}_w, \quad \mathbf{M}_h = \mathbf{M}_s + \mathbf{M}_w. \tag{10}$$

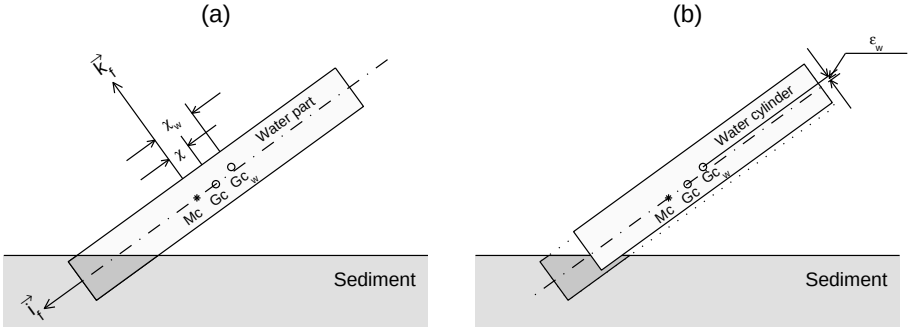

Fig. 3. Treatment of water-covered part for penetration of cylinder through the water-sediment interface: (a) original water-covered part, and (b) equivalent water-covered cylinder.

Hydrodynamic forcing from the sediment ($\mathbf{F}_s$, $\mathbf{M}_s$) can be integrated from the surface (σ) of the dry-cylinder and dry cut-off part,

$$\mathbf{F}_s = \iint_\sigma \mathbf{f}_s d\sigma, \quad \mathbf{M}_s = \iint_\sigma (\mathbf{r} \times \mathbf{f}_s) d\sigma \,, \tag{11}$$

where $\mathbf{f}_s$ is the hydrodynamic force exerted on the surface at the point **r** and represented in the m-coordinate. Let **v** be the velocity at point 'o' on the cylinder surface, and **n** be the normal unit vector (outward positive),

$$\mathbf{v} = \mathbf{V} + \mathbf{\Omega} \times \mathbf{r} \,.$$

The velocity (**v**) and hydrodynamic force (**f**) have normal and tangential components (Fig. 4),

$$\mathbf{f}_s = \mathbf{f}_s^{(n)} + \mathbf{f}_s^{(\tau)}, \quad \mathbf{v} = \mathbf{v}_n + \mathbf{v}_\tau \,. \tag{12}$$

Here, $\mathbf{f}_s^{(n)}$ and $\mathbf{f}_s^{(\tau)}$ are the resistant forces in the normal and tangential directions. Let *B*(z) and *S*(*z*) be the profiles of the sediment bulk density and shear strength. As an object moves in the sediment, the impact (resistant) force exerted on the part of the object's surface moving towards the sediment (Fig. 5),

$$\left|\mathbf{f}_s^{(n)}\right| = \left[p_{ws} + \int_{z_{ws}}^{z} B(z')dz' + S(z) \right] \delta \,, \tag{13}$$

where p_{ws} is the water pressure at the water-sediment interface, and δ is a step function

$$\delta = \begin{cases} 1 & \mathbf{v} \bullet \mathbf{n} \geq 0 \\ 0 & \mathbf{v} \bullet \mathbf{n} \leq 0 \end{cases}. \tag{14}$$

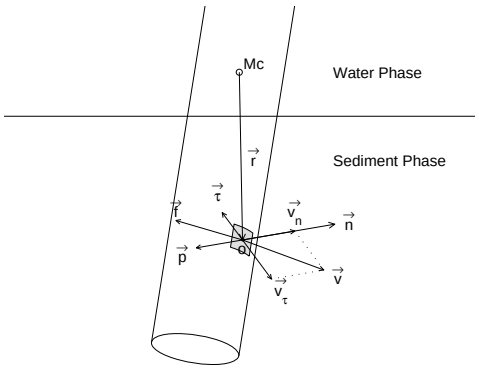

Fig. 4. Momentum and angular momentum balance for the penetration of rigid body through the water-sediment interface.

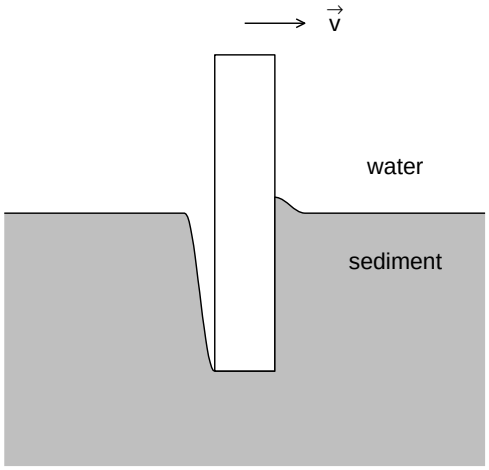

Fig. 5. The impact (resistant) force exerted on the part of the object's surface moving towards the sediment.

6. Cylinder Drop Experiments

Two cylinder drop experiments were conducted to collect data for the model evaluation. One was conducted at the Naval Postgraduate School (NPS) swimming pool in July 2001. It consisted of dropping cylinders into the water and recording the position as a function of time using two digital cameras at (30 Hz) as the cylinders fell 2.4 meters to the pool bottom. Detailed information can be found in Chu et al. (2002abc, 2003).

The other experiment was conducted on the R/V John Martin on May 23, 2000. The barrel with density ratio of 1.8 was released while touching the surface. This would be to eliminate any chance of inertial effects caused by uneven introduction into the air-sea interface. This also set the initial velocity parameter in the code to zero. The barrel was to be released 17 times. The diver would snap the quick-release shackle on the barrel and then dive down to conduct measurements. The average depth of the water was 13 meters. Since it was uncertain the path the barrel would follow, both the releasing diver and a second safety diver would stay on the surface until after the barrel had dropped. Once reaching the bottom, one diver would take penetration measurements using a meter stick marked at millimeter increments while the other would take a gravity core. After 17 drops, the divers

began to run out of air and results were not varying greatly so the decision was made to end the experiment. Upon return to the Monterey Bay Aquarium Research Institute, the gravity cores were taken immediately to the USGS Laboratories in Menlo Park, California where they were refrigerated until the analysis could be performed on May 31 – June 1, 2000.

7. Sediment Data Analysis

Analysis of the gravity cores was begun on May 31, 2000 at the USGS Laboratories in Menlo Park, California with the aid of a graduate student, Priscilla Barnes. The gravity cores were sliced into two-centimeter segments to a depth of ten centimeters, and then sliced into four-centimeter segments. A Fall Cone Apparatus (Model G-200) was used to determine sediment shear strength.

In the test, it is assumed that the shear strength of sediment at constant penetration of a cone is directly proportional to the weight of the cone and the relation between undrained shear strength s and the penetration h of a cone of weight Q is given by:

$$s = KQ / h^2 , \qquad (15)$$

where K is a constant which depends mainly on the angle of the cone, but is also influenced by the sensitivity of the clay/sediment. Four different cones are used with this instrument, each one having the measuring range listed in Table 1. The cones are suspended from a permanent magnet. By pressing a knob, the magnet is moved so that the magnetic field is broken momentarily, and the cone is released. Measurements are taken of penetration depth and the evolution is repeated five times per sediment slice. These values are then averaged and correlated with a table which gives shear strength.

TABLE 1 MEASUERING RANGES OF THE GRAVITY CORES

Weight(g)	**Apex-Angle**	**Penetration** (mm)	**Undrained shear strength** (kPa)
400	30°	4.0 – 15.0	25 – 1.8
100	30°	5.0 – 15.0	4 – 0.45
60	60°	5.0 – 15.0	0.6 – 0.067
10	60°	5.0 – 20.0	0.10– 0.0063

Previous studies (Chu et al. 2000a,b) showed that the sediment parameters are the most critical element in determining how deep an object was buried when it came to rest. During the experiment at the Monterey Bay, we obtained 17 gravity cores. Sediment bulk density and shear strength profiles (Fig. 6) show generally increase with depth until approximately 6-9 cm below the water-sediment interface.

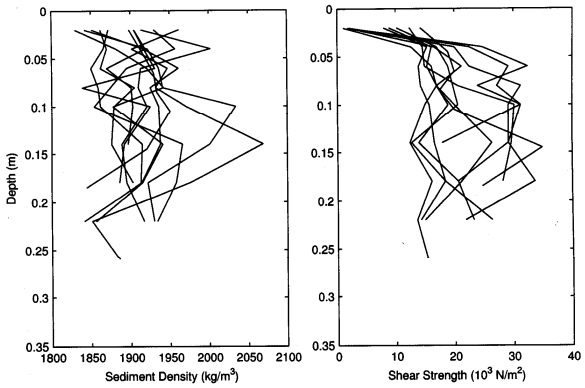

Fig. 6. Sediment density and shear strength profiles in the Monterey Bay collected during the cylinder drop experiment on May 31, 2000.

8. Model-Data Comparison

The U.S. Navy has a 2D model (Chu et al., 2000a, b) for mine (rigid object) impact burial prediction model. To evaluate the value-added of the newly developed 3D model (called IMPACT35), comparison among the observed and predicted using 2D and 3D models is conducted. After running the two models for each gravity core regime and location, the burial depths were compared with measured burial depth data (Fig. 7). As evident, IMPACT35 improves the prediction capability. The existing 2D model (IMPACT25) over predicts actual burial depth by an order of magnitude on average. However, the 3D model (IMPACT35) predicts the burial depth reasonably well. Since the gravity cores were taken for approximately two to three meters from the impact location, several cores were taken for each drop. This allowed an average to be calculated in order to yield more accurate data for each drop.

9. Conclusions

(1) IMPACT35 is developed to predict the translation and orientation of falling rigid body through air, water, and sediment. It contains three components: triple coordinate transform, hydrodynamics of falling rigid object in a single medium (air, water, or sediment) and in multiple media (air-water and water-sediment interfaces). The body and buoyancy forces and their moments in the E-coordinate system, the hydrodynamic forces (such as the drag and lift forces) and their moments in the F-coordinate, and the cylinder's moments of gyration in the M-coordinate.

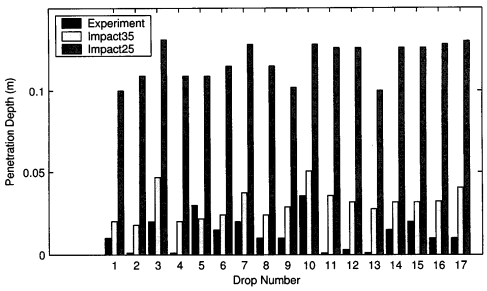

Fig. 7. Comparison among observed and predicted burial depths.

(2) The momentum (moment of momentum) equation for predicting the cylinder's translation velocity (orientation) is represented in the E-coordinate (M-coordinate) system. Transformations among the three coordinate systems are used to convert the forcing terms into E-coordinate (M-coordinate) for the momentum (moment of momentum) equation.

(3) Two cylinder drop experiments were conducted to evaluate the 3D model. Model-data comparison shows that IMPACT35 improves the prediction capability.

Acknowledgments

The Office of Naval Research Marine Geosciences Program (N0001403WR20178), Naval Oceanographic Office, and the Naval Postgraduate School supported this study.

References

Chu. P.C., V.I. Taber, and S.D. Haeger, AA mine impact burial model sensitivity study, Institute of Joint Warfare Analysis, Naval Postgraduate School, Technical Report, NPS-IJWA-00-003, pp.48, 2000a.

Chu, P.C., V. Taber, and S. Haeger, AEnvironmental sensitivity study on mine impact burial prediction model, Proceedings on The Fourth International Symposium on Technology and the Mine Problem, 10 pages, 2000b.

Chu, P.C., A.F. Gilles, C.W. Fan, J. Lan, and P. Fleischer, 2002a: Hydrodynamics of falling cylinder in water column. Advances in Fluid Mechanics, 4, 163-181.

Chu, P.C., T.B. Smith, and S.D. Haeger, 2002b: Mine impact burial prediction experiment. Journal of Counter-Ordnance Technology (CD Rom).

Chu, P.C., A.F. Gilles, C.W. Fan, and P. Fleischer, 2002c: Hydrodynamics of falling mine in water column. Journal of Counter-Ordnance Technology (CD Rom).

Chu, P.C., C.W. Fan, A.D. Evans, and A. Gilles, 2003: Triple coordinate transforms for prediction of falling cylinder through the water column. Journal of Applied Mechanics, in press.